Theoretical Study of the Electronic Spectroscopy of Peptides. 1. The Peptidic Bond: Primary, Secondary, and Tertiary Amides

Luis Serrano-Andrés* and Markus P. Fülscher

Contribution from the Department of Theoretical Chemistry, Chemical Centre, University of Lund, P.O.B. 124, S-221 00 Lund, Sweden

Received June 13, 1996. Revised Manuscript Received October 1, 1996[⊗]

Abstract: With the general aim to characterize the origin of electronic spectra of proteins, the present paper discusses the absorption spectra of a series of simple amides. Excited states were studied by means of *ab initio* quantum chemical methods—the Complete Active Space (CAS) SCF method and multiconfigurational second order perturbation theory (CASPT2). We calculated the vertical absorption spectra of three primary amides (formamide, acetamide, and propanamide), two secondary amides (*N*-methylformamide and *N*-methylacetamide), and one tertiary amide (*N*,*N*-dimethylformamide). The calculations comprise a large number of singlet and triplet valence and Rydberg excited states. The results support a basic structure of the spectra: In gas phase one intense valence $\pi \rightarrow \pi^*$ transition is placed between 6.5 and 7.4 eV and a second weak valence $\pi \rightarrow \pi^*$ transition occurs at 9.6−10.5 eV. Alkyl substitutions on the nitrogen have a major effect on the valence transitions: The energy drops when going from primary to secondary and tertiary amides. In contrast, only minor blue shifts of the excitation energies are observed when alkyl groups of different length are attached to the carboxyl group. For all molecules studied in this paper, $n \rightarrow \pi^*$ transitions from the oxygen lone pair are found at about 5.5 eV and reveal only small sensitivity on the length of the alkyl substituent.

1. Introduction

Absorption spectra of proteins can be considered as a superposition of spectra of individual chromophores. Because all experimentally easily accessible characteristic electronic transitions occur in a narrow energy region, the interpretation of the spectra is difficult. Typically, spectra consist of broad overlapping bands due to band broadening in solutions and crystal environments. Detailed knowledge of electronic properties of the monomers is important for the interpretation of electronic spectra of proteins.[1] For these reasons we have undertaken a project aiming for the accurate determination of $\pi \rightarrow \pi^*$ and $n \rightarrow \pi^*$ excitation energies and transition moments of chromophores in proteins.

Electronic spectra of proteins can be mainly attributed to three groups of chromophores: histidine and the aromatic amino acids tryptophan, phenylalanine, and tyrosine; the peptide bond or amide chromophore, as it is usually named; and the terminal carboxylic acid and amine groups. They all possess characteristic spectra. Earlier, we have presented calculations on the first group of chromophores. In these studies the aromatic side chains were modeled by benzene, phenol, and indole, respectively.[2,3] Imidazole was computed to account for the spectrum of histidine.[2,4] In this paper we report electronic properties of the amide group as modeled by formamide. To mimic the effect of a protein chain on the spectra we also investigated a number of alkylated derivatives of formamide. In a subsequent paper we will discuss the electronic properties of terminal amino and carboxyl groups and, finally, we will also propose a new interpretation of the absorption spectra of proteins based on model calculations on dipeptides.

The electronic spectra of proteins can also be divided into three ranges of absorption energies. Region I includes low-energy transitions and extends to nearly 5.0 eV. Range II extends from 5.6 to 6.5 eV and, typically, exposes a complex band structure. Finally, the high-energy range III includes the far UV and starts at about 6.5 eV. Aromatic amino acids, if present, give clear and characteristic absorption maxima in regions I and II. In previous studies we computed the spectra of the latter molecules and explained their absorption spectra as the result of four main $\pi \rightarrow \pi^*$ valence singlet states and transitions: ^1L_b, ^1L_a, ^1B_b, and ^1B_a.[2,3] The lowest state in each of the molecules (two in indole) is responsible for the weak transition observed below 5.0 eV, while those remaining appear in the 5.6−6.5 eV region as intense bands. The amino acid histidine—modeled by its imidazole fragment—does not match this picture because of the less aromatic character. The four valence transitions lie in this case higher in energy, from 6.0 to 8.5 eV.[4] The second and third types of chromophores in proteins, the peptidic bond or amide chromophore as well as terminal amino and carboxyl groups, absorb at the edge of region II and in region III.

From qualitative theoretical considerations, one may expect the electronic excitation epectrum of simple amides in the gas phase to include one $n \rightarrow \pi^*$, two $\pi \rightarrow \pi^*$ valence, and a number of Rydberg transitions. In addition, one may also observe some very weak $\sigma-\pi^*$ transitions.[5] By comparison of the few lowest ionization potentials of formamide and formaldehyde[5,6] and considering also the calculations on

[⊗] Abstract published in *Advance ACS Abstracts,* November 1, 1996.

(1) Demchenko, A. P. *Ultraviolet Spectroscopy of Proteins*; Springer-Verlag: Berlin, 1986.

(2) Roos, B. O.; Andersson, K.; Fülscher, M. P.; Malmqvist, P.-Å.; Serrano-Andrés, L.; Pierloot, K.; Merchán, M. In *Advances in Chemical Physics: New Methods in Computational Quantum Mechanics*; Prigogine, I., Rice, S. A., Eds.; John Wiley & Sons: New York, 1996; Vol. XCIII, p 219.

(3) Serrano-Andrés, L.; Roos, B. O. *J. Am. Chem. Soc.* **1996**, *118*, 185.

(4) Serrano-Andrés, L.; Fülscher, M.; Roos, B. O.; Merchán, M. *J. Chem. Phys.* **1996**, *100*, 6484.

(5) Robin, M. B. *Higher Excited States of Polyatomic Molecules*; Academic Press: New York, 1975; Vol. II.

(6) Lisini, A.; Keane, M. P.; Lunell, S.; Correia, N.; de Brito, A. N.; Svensson, S. *Chem. Phys.* **1993**, *169*, 379.

S0002-7863(96)01996-8 CCC: $12.00

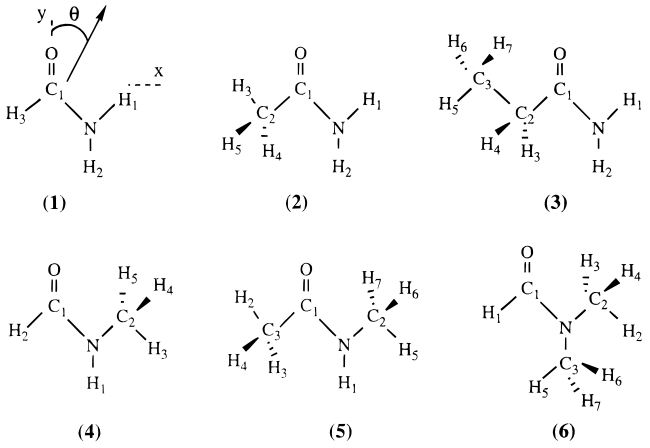

Figure 1. Structure and atom labeling of the amides (C_s symmetry): (**1**) formamide; (**2**) acetamide; (**3**) propanamide; (**4**) *N*-methylformamide; (**5**) *N*-methylacetamide; (**6**) *N*,*N*-dimethylformamide. The arrow defines the positive angles (θ) of the transition moment directions.

formaldehyde[7,8] as well as the spectra of isoelectronic systems such as butadiene or acrolein, one arrives at the following qualitative picture: An n $\rightarrow \pi^*$ transition is likely to be observed close to 5 eV and the $\pi \rightarrow \pi^*$ excitation energies may be close to 7 and 9 eV, respectively. Recently, Clark[9] reported the polarized vacuum UV absorption spectra of single crystals to propanamide. Two prominent bands, around 6.9 and 9.9 eV, were observed. Furthermore, a weak transition was identified at about 7.5 eV and assigned to a Rydberg state.

Clark's view of the spectrum of propanamide is in accord with the exceptions outlined above, but it is in conflict with earlier assignments: The gas-phase spectra of the simple amides have been interpreted as five-band systems including transitions named, according to Mulliken's nomenclature, W, R_1, NV_1, R_2, and Q states. In 1953 Hunt and Simpson[10] reported ultraviolet spectra for some simple amides. Originally, these authors assumed that the two valence $\pi \rightarrow \pi^*$ bands in formamide, named NV_1 and NV_2, were placed around 7.2 and 9.2 eV, respectively. However, Hunt and Simpson also studied *N*,*N*-dimethylformamide which exposes a new band at about 7.7 eV. To explain its origin Hunt and Simpson assumed that the second $\pi \rightarrow \pi^*$ transition had shifted as much as 1.5 eV to lower energies upon alkyl substitution. Four years later Peterson and Simpson[11] reported the electronic spectrum of myristamide in crystalline phase. In accord with previous work they considered the 6.7- and 7.7-eV bands to be due to $\pi \rightarrow \pi^*$ excited valence states. Despite, contradictory reports,[5] the assignment of the 7.5-eV band survived (compare with ref 1).

The present paper focuses on absorption spectra of a series of simple amides in order to determine the optical properties of the isolated peptide bond. To this end we calculated the gas-phase spectra of the primary amides formamide, acetamide, and propanamide, the secondary amides *N*-methylformamide and *N*-methylacetamide, and the tertiary amide *N*,*N*-dimethylformamide (see Figure 1). This study includes valence and Rydberg, singlet and triplet excited states at the ground state equilibrium geometry. The calculations have been performed using the CASSCF/CASPT2 method. This approach has proven to be especially suited to deal with excited states of conjugated and aromatic organic molecules.[2,12] Our calculations reproduce known excitation energies with an accuracy better than 0.2 eV and give full support to Robin's and Clark's view on the electronic properties of the peptide bond.

2. Methods and Computational Details

The ground-state geometries of the present molecules were optimized at the MP2 level using the 6-31G* basis set. The optimization was restricted to keep C_s symmetry. On the one hand, this assumption can be justified recalling that the carbon skeleton of the present molecules has proven to be almost planar in different environments, both in experimental[9,13] and in earlier theoretical[14,15] studies. On the other hand, the Hessian of the C_s MP2/6-31G* optimized geometries indicates that these structures are in fact not global minima. The molecules tend to lose their planarity. However, additional MP2 geometry optimizations for formamide using cc-pVDZ and cc-pVTZ basis sets[16] seem to indicate that the nonplanarity is due to basis set size. If the cc-pVTZ basis sets are used one finally obtains a planar C_s structure with bond distances and angles similar to the 6-31G* geometry (we tested it for formamide and acetamide).

It has been shown[17,18] that calculations of electronic spectra require extended basis sets. Therefore, ANO-type basis sets[19] were used and contracted to TZP quality for C, N, and O (C,N,O 4s3p1d/H 2s). These were supplemented with a 1s1p1d set of Rydberg-type functions (contracted from 8 primitives for each angular momentum type), which were built following the procedure described earlier.[12] The additional functions were computed independently for each molecule and placed at the average charge centroid of both the $^2A'$ and $^2A''$ cations. This procedure has proven to yield accurate descriptions of both valence and Rydberg excited states in a number of earlier applications.[12] The carbon and nitrogen 1s electrons were kept frozen in the form determined by the ground-state SCF wave function and were not included in the calculation of the correlation energy.

The CASSCF/CASPT2 method[2,20,21] is a two-step procedure and calculates the first-order corrected wave function and the second-order energy with a CASSCF wave function constituting the reference function. Thus, initially the multiconfigurational wave functions are determined at the CASSCF level of approximation[22] and are used to calculate molecular properties. The CAS State Interaction method (CASSI) is then used to compute transition properties[25] and transition moments. Finally, the dynamic correlation energy contributions to the state energies are obtained by the second-order perturbation treatment. Recently, a level shift technique has been introduced,[23,24] the socalled LS-CASPT2 approach, which allows the effect of intruder states common in many calculations on excited states to be avoided. Here, a value of 0.3 au has been used for the level shift in all the computed states.

(7) Merchán, M.; Roos, B. O. *Theor. Chim. Acta* **1995**, *92*, 227.
(8) Gwaltney, S. R.; Bartlett, R. J. *Chem. Phys. Lett.* **1995**, *241*, 26.
(9) Clark, L. B. *J. Am. Chem. Soc.* **1995**, *117*, 7974.
(10) Hunt, H. D.; Simpson, W. T. *J. Am. Chem. Soc.* **1953**, *75*, 4540.
(11) Peterson, D. L.; Simpson, W. T. *J. Am. Chem. Soc.* **1957**, *79*, 2375.
(12) Roos, B. O.; Fülscher, M. P.; Malmqvist, P.-Å.; Merchán, M.; Serrano-Andrés, L. In *Quantum Mechanical Electronic Structure Calculations with Chemical Accuracy*; Langhoff, S. R., Ed.; Kluwer Academic Publishers: Dordrecht, The Netherlands, 1995; p 357.
(13) Kydd, R. A.; Dunham, A. R. *J. Mol. Struct.* **1980**, *69*, 79.
(14) Schnur, D. H.; Yuh, Y. H.; Dalton, D. R. *J. Org. Chem.* **1989**, *54*, 3779.
(15) Gao, J. *J. Am. Chem. Soc.* **1993**, *115*, 2930.
(16) Dunning, T. H. *J. Chem. Phys.* **1989**, *90*, 1007.
(17) Fülscher, M. P.; Roos, B. O. *Theor. Chim. Acta* **1994**, *87*, 403.
(18) Fülscher, M. P.; Roos, B. O. *J. Am. Chem. Soc.* **1995**, *117*, 2089.
(19) Widmark, P.-O.; Malmqvist, P.-Å.; Roos, B. O. *Theor. Chim. Acta* **1990**, *77*, 291.
(20) Andersson, K.; Malmqvist, P.-Å.; Roos, B. O.; Sadlej, A. J.; Wolinski, K. *J. Phys. Chem.* **1990**, *94*, 5483.
(21) Andersson, K.; Malmqvist, P.-Å.; Roos, B. O. *J. Chem. Phys.* **1992**, *96*, 1218.
(22) Roos, B. O. In *Advances in Chemical Physics: Ab Initio Methods in Quantum Chemistry*; Lawley, K. P., Ed., John Wiley & Sons Ltd.: Chichester, England, 1987; Vol. II, Chapter 69, p 399.
(23) Roos, B. O.; Andersson, K. *Chem. Phys. Lett.* **1995**, *245*, 215.
(24) Roos, B. O.; Andersson, K.; Fülscher, M. P.; Serrano-Andrés, L.; Pierloot, K.; Merchán, M.; Molina, V. *J. Mol. Struct. (Theochem)* **1996**, in press.
(25) Malmqvist, P. Å.; Roos, B. O. *Chem. Phys. Lett.* **1989**, *155*, 189.
(26) Andersson, K.; Fülscher, M. P.; Karlström, G.; Lindh, R.; Malmqvist, P.-Å.; Olsen, J.; Roos, B. O.; Sadlej, A. J.; Blomberg, M. R. A.; Siegbahn, P. E. M.; Kellö, V.; Noga, J.; Urban, M.; Widmark, P.-O. *MOLCAS Version 3*; Department of Theoretical Chemistry, Chemistry Center, University of Lund, P.O.B. 124, S-221 00 Lund, Sweden, Lund, 1994.

Table 1. Calculated and Experimental Excitation Energies (eV), Oscillator Strengths, Dipole Moments μ (D), Spatial Extension $\langle r^2 \rangle$ (au), and Transition Moment Directions (deg) for the Excited Singlet and Triplet States in Formamide

	excitation energies						oscil str			TM_{dir}[a]
state	CAS	PT2	exp[b]	CI[c]	μ	$\langle r^2 \rangle$	tw[g]	exp	CI[c]	tw[g]
$1^1A'$(G.S.)					4.08	39				
$1^1A''$(n → π^*)	8.30	5.61	5.5[d]	5.86	2.12	38	0.001	0.002[e]	0.0003	
$2^1A''$(2a″ → 3s)	7.47	6.52	6.5	6.14	4.00	75	0.024		0.022	
$2^1A'$(10a′ → 3s)	8.01	6.59	6.8	6.49	3.67	72	0.003		0.0004	−33
$3^1A''$(2a″ → $3p_y$)	8.32	7.04	7.1	7.01	1.70	70	0.0001		0.0005	
$3^1A'$(10a′ → $3p_y$)	8.65	7.31	7.3	7.16	0.59	76	0.065		0.060	+28
$4^1A'$(π → π^*)	8.83	7.41	7.4	7.94	6.12	39	0.371	0.30[e]	0.149	−32
$5^1A'$(2a″ → $3p_z$)	8.83	7.72	7.7	7.40	4.06	80	0.101		0.136	−45
$6^1A'$(10a′ → $3p_x$)	9.03	7.73	7.9	7.50	4.05	78	0.022		0.041	+34
$4^1A''$(10a′ → $3p_z$)	9.24	7.81		7.47	2.09	73	0.005		0.005	
$5^1A''$(2a″ → $3p_x$)	8.91	7.97		7.57	6.31	76	0.007		0.005	
$7^1A'$(2a″ → $3d_{xz}$)	9.65	8.02	8.1		4.59	62	0.087			−46
$8^1A'$ (10a′ → $3d_{z^2}$)	10.28	8.94	8.8		3.49	70	0.002			+1
$6^1A''$(2a″ → $3d_{z^2}$)	9.95	8.98	9.1		4.93	67	0.002			
$9^1A'$(10a′ → $3d_{x^2-y^2}$)	10.45	9.17	9.2		3.54	75	0.011			−16
$10^1A'$(10a′ → $3d_{xy}$)	10.57	9.26			7.41	77	0.005			+76
$7^1A''$(2a″ → $3d_{x^2-y^2}$)	10.24	9.32	9.3		7.74	74	0.018			
$8^1A''$(10a′ → $3d_{xz}$)	11.14	9.43			3.07	70	0.006			
$9^1A''$(2a″ → $3d_{xy}$)	10.42	9.47	9.5		11.30	78	0.017			
$10^1A''$(10a′ → $3d_{yz}$)	10.78	9.54			4.46	71	0.001			
$11^1A'$(2a″ → $3d_{yz}$)	11.03	9.80	9.8		6.52	74	0.030			−38
$11^1A''$(1a″ → 3s)	11.01	9.93	9.9		4.70	75	0.034			
$12^1A'$(π → π^*)	11.93	10.50			5.24	40	0.131	0.1[e]		+57
$1^3A''$(n → π^*)	6.72	5.34	5.30[f]		1.39	38				
$1^3A'$(π → π^*)	7.05	5.69			3.23	38				
$2^3A''$(2a″ → 3s)	6.84	6.30			3.06	72				
$2^3A'$(10a′ → 3s)	7.29	6.61			3.62	71				

[a] The molecule is placed in the *xy* plane (C_s symmetry). The convention used places the *y* axis along the CO bond and the nitrogen in the fourth quadrant. The positive angles are defined clockwise from the *y* axis in the first quadrant as in ref 9. See Figure 1. [b] Vacuum transitions for formamide, refs 10 and 28. [c] CASSCF/MRCI 6-31G** results, ref 31. [d] Estimated value for acetamide in nonpolar solvents. In water the band appears near 5.9 eV. References 9 and 34. [e] Estimated values in solution. References 9 and 34. [f] Trapped electron spectrum of formamide in the gas phase. Reference 30. [g] This work.

The selection of the proper active space is the crucial step in the CASSCF/CASPT2 approach. In general, the active space should include all orbitals with occupation numbers appreciably different from two or zero in any of the excited states under consideration. This means that all near-degeneracy effects are included in the CASSCF reference function, and consequently there will be no large terms in the perturbation expansion. To compute the electronic π spectrum in the studied molecules the active space should initially include the three π,π^* orbitals and the σ lone pair orbital on the oxygen, together with the 6 corresponding electrons. This is the minimal space for calculations on the valence π-electron spectrum. In addition, one more σ orbital is included in the active space to account for $\sigma \rightarrow \sigma^*$ excitations and one more π orbital which is used as as additional correlating orbital for the π space, where only one valence π^* orbital is present. The final valence space can be labeled (2,4), representing the number of a′ and a″ orbitals, respectively, of the active space in the C_s framework.

In numerous calculations we have shown[12] that a valence basis set and a valence active space do not guarantee that the obtained states have a pure valence character. Rydberg states may interact with valence states. A restricted selection of basis sets and active space usually leads to erratic results since Rydberg states often appear among the valence excited states. The recommended procedure is therefore to always include diffuse functions in the basis set and Rydberg-type orbitals in the active space. To compute the lowest (3s, 3p, and 3d) Rydberg series we should include nine additional orbitals, six of a′ symmetry and three of a″ symmetry. This leads to a large active space of 6 electrons in 15 orbitals, and is at the limit of the employed CASSCF program. For the sake of clarity and to prove the small sensitivity to the CASSCF/CASPT2 approach to the size of the active space, we decided to carry out the calculations on formamide with this large active space, labeled (8,7). One single CASSCF calculation including 15 CASSCF averaged roots (equal weight) for the $^1A'$ states and one calculation including 11 roots for the $^1A''$ states contains simultaneously all the expected valence and Rydberg singlet states which are given in Table 1. The valence states were then re-computed in an additional calculation where the 9 Rydberg orbitals were removed from the active space (see below).

Calculations including 15 active orbitals and 11 roots are expensive. For the larger molecules we decided, therefore, to use a smaller active space. We consider first only the 3s and 3p Rydberg orbitals, and, hence, three a′ orbitals and one a″ orbital are needed to the valence active space, resulting in a total active space labeled (5,5). All calculations needed to characterized the 3s and 3p Rydberg states are carried out, and, finally, the 3s and 3p Rydberg orbitals are removed from the orbital space. In successive steps the 3d Rydberg orbitals take their place and the process is reiterated. Finally, the valence state properties are determined from CASSCF wave functions where all Rydberg orbitals were removed from the active space. As shown by the results for formamide the states can be computed without any notable loss of quality: The excitation energies differ by less than 0.05 eV as compared to the calculations using the (8,7) active space. On the other hand, the simultaneous computation of valence and Rydberg states at the CASSCF level leads to a strong mixing between states of valence and Rydberg character. The effect on the computed excitation energies is, in general, small for Rydberg states but large for the valence states. Earlier, it has been observed that the procedure described above, to a large extend, avoids such mixings and has been applied successfully[2,3,12,18] earlier.

The calculations have been performed with the MOLCAS-3[26] program package on IBM RS/6000 workstations except for the MP2 optimizations which used the MULLIKEN[27] program.

3. Results and Discussion

The following sections describe the computed results and suggest assignments for the singlet and triplet valence and Rydberg states of the studied primary, secondary, and tertiary amides, respectively. Tables 1−6 list the computed excitation energies, dipole moments, spatial extensions, oscillator strengths, and transition moment directions in the gas phase and also

Table 2. Calculated and Experimental Excitation Energies (eV), Oscillator Strengths, Dipole Moments μ (D), Spatial Extension $\langle r^2 \rangle$ (au), and Transition Moment Directions (deg) for the Excited Singlet and Triplet States in Acetamide

	excitation energies					oscil str		TM dir[a]
state	CAS	PT2	exp	μ	$\langle r^2 \rangle$	tw[g]	exp	tw[g]
$1^1A'$(G.S.)				4.00	52			
$1^1A''$(n $\rightarrow \pi^*$)	7.19	5.54	5.44[c]	2.19	50	0.001	0.002[f]	
$2^1A''$(3a″ $\rightarrow$ 3s)	7.11	6.38		4.11	94	0.022		
$2^1A'$(13a′ $\rightarrow$ 3s)	7.60	6.40	6.45[d]	3.98	95	0.018	0.02[b]	+80
$3^1A''$(13a′ $\rightarrow$ $3p_z$)	8.72	7.02		1.43	102	0.001		
$3^1A'$(3a″ $\rightarrow$ $3p_z$)	8.23	7.14		2.40	126	0.060		−37
$4^1A'(\pi \rightarrow \pi^*)$	11.28	7.21	7.4[e]	6.21	55	0.292	0.21[f]	−31
$5^1A'$(13a′ $\rightarrow$ $3p_x$)	8.42	7.35		3.06	135	0.013		−26
$6^1A'$(13a′ $\rightarrow$ $3p_y$)	8.37	7.38		1.60	133	0.009		+69
$4^1A''$(3a″ $\rightarrow$ $3p_y$)	8.17	7.53		2.82	134	0.00001		
$5^1A''$(3a″ $\rightarrow$ $3p_x$)	8.44	7.73	7.6[e]	7.89	127	0.004		
$7^1A'$(13a′ $\rightarrow$ $3d_{z^2}$)	9.36	8.01		12.18	210	0.0001		−33
$8^1A'$(13a′ $\rightarrow$ $3d_{x^2-y^2}$)	9.40	8.05	7.9[e]	13.41	216	0.006		+8
$9^1A'$(13a′ $\rightarrow$ $3d_{xy}$)	9.45	8.12		11.78	222	0.002		+71
$6^1A''$(13a′ $\rightarrow$ $3d_{yz}$)	9.04	8.20		8.88	228	0.0001		
$7^1A''$(13a′ $\rightarrow$ $3d_{xz}$)	9.04	8.23		11.17	213	0.0001		
$10^1A'$(3a″ $\rightarrow$ $3d_{yz}$)	9.43	8.48		10.08	226	0.007		+30
$8^1A''$(3a″ $\rightarrow$ $3d_{z^2}$)	8.89	8.49		13.83	208	0.004		
$11^1A'$(3a″ $\rightarrow$ $3d_{xz}$)	9.52	8.55		16.15	216	0.014		−28
$9^1A''$(3a″ $\rightarrow$ $3d_{x^2-y^2}$)	8.98	8.60		19.05	205	0.0001		
$10^1A''$(3a″ $\rightarrow$ $3d_{xy}$)	9.05	8.64		19.98	204	0.00001		
$11^1A''$(2a″ $\rightarrow$ 3s)	10.53	9.47		5.07	95	0.027		
$12^1A'(\pi \rightarrow \pi^*)$	12.93	10.08	9.9[b]	5.15	61	0.179	0.1[b]	+50
$1^3A''$(n $\rightarrow \pi^*$)	6.23	5.24		1.61	53			
$1^3A'(\pi \rightarrow \pi^*)$	7.41	5.57		3.81	58			
$2^3A''$(3a″ $\rightarrow$ 3s)	6.81	6.21		4.10	90			
$2^3A'$(13a′ $\rightarrow$ 3s)	7.21	6.37		4.11	94			

[a] The molecule is placed in the *xy* plane (C_s symmetry). The convention used places the *y* axis along the CO bond and the nitrogen in the fourth quadrant. The positive angles are defined clockwise from the *y* axis in the first quadrant as in ref 9. See Figure 1. [b] Data from the crystal spectrum of propanamide. Reference 9. [c] Estimated value in dioxane. In water the band appears near 5.9 eV. Reference 34. [d] In-plane polarized transition in the gas phase. References 9 and 35. [e] Vacuum transition, ref 28. In water the $\pi \rightarrow \pi^*$ band appears at 6.81 eV, refs 34 and 35. [f] Estimated values in solution. References 9 and 34. [g] This work.

include the comparison to available experimental data. The effects of the elongation of the alkyl group attached to the carbon of the amide group and the alkyl substitution on the nitrogen on the transitions and the relation to the polyamides spectra are finally discussed in a separate section.

1. Primary Amides: Formamide, Acetamide, and Propanamide. A detailed gas-phase spectrum of formamide up to 10.0 eV was reported by Hunt and Simpson.[10] The spectrum exhibits a strong broad band centered around 7.4 eV which is superimposed by a number of sharp peaks. Moreover, two weak bands appear at 6.5 and 6.8 eV. The gas-phase spectrum reported by Kaya and Nagakura[28] up to 8.1 eV is essentially identical, although the bands observed between 7.7 and 8.8 eV are less sharp. In Table 1 we included tentative assignments of the observed bands. The n $\rightarrow \pi^*$ band computed at 5.61 eV is apparently not observed in the experimental spectra, although its presence can be inferred in Hunt and Simpson's spectrum below 6.0 eV. The weak bands observed at 6.5 and 6.8 eV have been assigned to the beginning of the Rydberg series HOMO $\pi \rightarrow$ 3s and n $\rightarrow$ 3s, respectively. The former transition should be more intense as indicated by the oscillator strength, but both bands have similar intensities in the spectrum. Between 7.2 and 7.4 eV the spectrum presents several bands with high intensity. We have tentatively assigned the broadest band at 7.4 eV to the valence $\pi \rightarrow \pi^*$ NV_1 band computed at 7.41 eV with an oscillator strength of 0.371. A detailed study of the vibrational transitions would be needed to solve the assignments unambiguously. The second valence $\pi \rightarrow \pi^*$ transition is computed at 10.50 eV with an oscillator strength of 0.131. No experimental data are available at such high energies for formamide. We have also performed calculations trying to locate the low-lying n $\rightarrow \sigma^*$ and $\pi \rightarrow \sigma^*$ transitions but they appeared at energies higher than 10.5 eV.

The rich band structure of the reported formamide spectrum in the gas phase makes it possible to assign a large number of Rydberg states. The computed Rydberg states are characterized throughout by relatively large intensities and energy separations. Such a behavior appears to be common to small and flexible molecules such as formamide.[29] On the low-energy side of the valence band, we have assigned the shoulder at 7.1 and 7.3 eV to the $3^1A''$ (2a″ $\rightarrow$ $3p_y$) and $3^1A'$ (10a′ $\rightarrow$ $3p_y$) states, respectively. Moreover, three clear and sharp peaks are observed in the spectrum at 7.7, 7.9, and 8.1 eV. For reasons of consistency (see section 3.4) the first two bands were assigned to the $5^1A'$ (2a″ $\rightarrow$ $3p_z$) and $6^1A'$ (10a′ $\rightarrow$ $3p_x$) states, respectively. The 8.1-eV band can be easily assigned to the $7^1A''$ (10a′ $\rightarrow$ $3d_{xz}$) state computed at 8.02 eV and an intensity of 0.087 eV. In the vertical absorption spectrum of formamide, at the ground state geometry, the n $\rightarrow \pi^*$ triplet state lies 0.35 eV below the $\pi \rightarrow \pi^*$ triplet state computed in the other amides. An experimental value of 5.30 eV is reported for the lowest vertical transition to a triplet state[30] which is in perfect agreement with the computed value, 5.28 eV.

(27) Rice, J. E.; Horn, H.; Lengsfield, B. H.; McLean, A. D.; Carter, J. T.; Replogle, E. S.; Barnes, L. A.; Maluendes, S. A.; Lie, G. C.; Gutowski, M.; Rudge, W. E.; Sauer, S. P. A.; Lindh, R.; Andersson, K.; Chevalier, T. S.; Widmark, P.-O.; Bouzida, D.; Pacanski, G.; Singh, K.; Gillan, C. J.; Carnevali, P.; Swope, W. C.; Liu, B. *MULLIKEN Version 1.1.0*; Almaden, Research Center, IBM Research Division, 6500 Harry Road, San Jose, CA, 95120-6099, 1994.

(28) Kaya, K.; Nakagura, S. *Theor. Chim. Acta* **1967**, *7*, 117.

(29) Serrano-Andrés, L.; Merchán, M.; Nebot-Gil, I.; Lindh, R.; Roos, B. O. *J. Chem. Phys.* **1993**, *98*, 3151.

(30) Staley, R. H.; Harding, L. B.; Goddard, W. A., III; Beauchamp, J. L. *Chem. Phys. Lett.* **1975**, *36*, 589.

Table 3. Calculated and Experimental Excitation Energies (eV), Oscillator Strengths, Dipole Moments μ (D), Spatial Extensions $\langle r^2 \rangle$ (au), and Transition Moment Directions (deg) for the Excited Singlet and Triplet States in Propanamide

	excitation energies					oscil str		TM dir[a]	
state	CAS	PT2	Exp	μ	$\langle r^2 \rangle$	tw[h]	exp	tw[h]	exp[b]
$1^1A'$(G.S.)				4.13	68				
$1^1A''(n \rightarrow \pi^*)$	8.27	5.48	5.44[c]	1.90	63	0.001	0.002[f]		
$2^1A''(4a'' \rightarrow 3s)$	7.06	6.38		4.68	114	0.022			
$2^1A'(16a' \rightarrow 3s)$	7.55	6.42	6.5[d]	5.00	116	0.019	0.02[b]	+75	−38 (+4)
$3^1A''(16a' \rightarrow 3p_z)$	8.68	6.94		1.35	117	0.001			
$3^1A'(4a'' \rightarrow 3p_z)$	8.22	7.19		2.36	146	0.052		−30	
$4^1A'(\pi \rightarrow \pi^*)$	10.44	7.28	7.4[e]	5.59	66	0.346	0.21[f]	−31	−35
$5^1A'(16a' \rightarrow 3p_x)$	8.32	7.34		4.28	154	0.011		−86	
$6^1A'(16a' \rightarrow 3p_y)$	8.42	7.35		4.28	155	0.008		−13	
$4^1A''(4a'' \rightarrow 3p_y)$	8.16	7.55		0.83	154	0.0001			
$5^1A''(4a'' \rightarrow 3p_x)$	8.43	7.71	7.7[g]	9.54	139	0.004			
$7^1A'(16a' \rightarrow 3d_{xy})$	8.95	8.11		11.46	253	0.002		+31	
$8^1A'(16a' \rightarrow 3d_{z^2})$	8.95	8.13		16.83	241	0.001		−53	
$9^1A'(16a' \rightarrow 3d_{x^2-y^2})$	9.00	8.14	8.0[g]	20.45	245	0.001		+75	
$6^1A''(16a' \rightarrow 3d_{yz})$	8.82	8.18		13.71	257	0.002			
$7^1A''(16a' \rightarrow 3d_{xz})$	9.01	8.25		13.38	249	0.001			
$8^1A''(4a'' \rightarrow 3d_{z^2})$	8.92	8.53		13.96	248	0.0001			
$10^1A'(4a'' \rightarrow 3d_{yz})$	9.01	8.58		12.27	255	0.010		−5	
$11^1A'(4a'' \rightarrow 3d_{xz})$	9.29	8.59		20.66	246	0.012		+70	
$9^1A''(4a'' \rightarrow 3d_{x^2-y^2})$	9.02	8.62		22.02	237	0.001			
$10^1A''(4a'' \rightarrow 3d_{xy})$	9.05	8.64		25.28	217	0.001			
$11^1A''(3a'' \rightarrow 3s)$	10.47	9.44		5.65	115	0.027			
$12^1A'(\pi \rightarrow \pi^*)$	13.31	9.95	9.9[b]	4.59	76	0.205	0.1[b]	+52	+46 (−72)
$1^3A''(n \rightarrow \pi^*)$	7.50	5.28		1.41	69				
$1^3A'(\pi \rightarrow \pi^*)$	7.18	5.94		2.47	64				
$2^3A'(16a' \rightarrow 3s)$	7.02	6.14		4.81	111				
$2^3A''(4a'' \rightarrow 3s)$	7.02	6.20		4.95	108				

[a] The molecule is placed in the *xy* plane (C_s symmetry). The convention used places the *y* axis along the CO bond and the nitrogen in the fourth quadrant. The positive angles are defined clockwise from the *y* axis in the first quadrant as in ref 9. See Figure 1. [b] Data from the crystal spectrum of propanamide. The alternative directions are given in parentheses. Reference 9. [c] Estimated value for acetamide in dioxane. In water the band appears near 5.7 eV. References 9 and 34. [d] Out-of-plane polarized transition in the gas phase. Reference 9. [e] Vacuum transition for acetamide, ref 28. In water the band appears at 6.89 eV for propanamide, refs 9 and 34. [f] Estimated values in solution. References 9 and 34. [g] Observed transition in crystal propanamide and myristamide. References 9 and 11. [h] This work.

A number of theoretical calculations on the electronic spectrum of formamide have been reported in the literature. Oliveros *et al*.[32] performed CIPSI calculations. The excitation energies for the lowest states were $^1A'$ $n \rightarrow \pi^*$ 5.85 eV and $^1A'$ $\pi \rightarrow \pi^*$ 7.56 eV. Sobolewski[33] also presented CASSCF/CASPT2 calculations ($^1A'$ $n \rightarrow \pi^*$ 5.85 eV; $^1A'$ $\pi \rightarrow \pi^*$ 7.67 eV). This author, however, completely disregarded Rydberg states and therefore did not include any additional functions in the basis sets. To disregard the Rydberg states leads, in our own experience, to an inadequate treatment of the valence states and differences in the excitation energies of ≈0.2 eV. Recently, Hirst *et al*.[31] reported CASSCF/MRCI calculations on formamide using 6-31G** basis sets. Those results are also shown in Table 1. We observe that Hirst *et al*. computed the NV_1 $\pi \rightarrow \pi^*$ state 0.54 eV too high in energy. Differences of 0.5 eV are common for truncated CI treatments. In addition, the Rydberg states seem to have been computed with too low energies. Lack of dynamical correlation and basis sets of poorer quality than those employed in our calculations could be possible factors for the discrepancy.

The gas-phase spectrum of acetamide reported by Kaya and Nagakura[28] shows an intense and broad band peaking at 7.4 eV and two shoulders at 7.6 and 7.8 eV. In solution the prominent band shifts to the red with increasing polarity of the solvent: 6.8 eV in water and around 6.9 eV in cyclohexane.[34,35] This shift is characteristic of $\pi \rightarrow \pi^*$ transitions. In addition, a weak transition in the red edge of the spectrum was observed at 5.9 eV in water and at 5.44 eV in dioxane.[35] The blue shift supports its $n \rightarrow \pi^*$ character.

The computed excitation energies for the first and second $\pi \rightarrow \pi^*$ valence excited states are 7.21 eV (NV_1) and 10.08 eV (NV_2). The excitation energies decreased as compared to formamide. The $n \rightarrow \pi^*$ singlet transition is computed at 5.54 eV. The result is in agreement with the experimental estimation in nonpolar solvents[34] at 5.44 eV. In addition, the dipole moment, 2.19 D, is almost half the value of the ground state, and therefore a large blue shift can be expected in polar solvents. Our calculations also allow the assignment of some Rydberg transitions. The two Rydberg series, $2a'' \rightarrow n = 3$ and $10a' \rightarrow n = 3$, present important changes with respect to those of the formamide. The splitting among the different members of the series decreased. A weak in-plane transition has often been reported for several amides around 6.5 eV, in both gas and solid phase.[9] This band can also be found in acetamide and corresponds to the $2^1A'(13a' \rightarrow 3s)$ transition computed at 6.40 eV. We also find a second out-of-plane transition, $2^1A''(3a'' \rightarrow 3s)$, close in energy and with similar intensity. In general, the intensity of the bands strongly decreases as compared to formamide and the acetamide spectrum does not show sharp peaks.

The spectrum of propanamide is similar to that of acetamide. The energy and intensity of the $\pi \rightarrow \pi^*$ NV_1 transition slightly increases as compared to acetamide (7.28 and 7.21 eV, respectively). The energy of the NV_2 transition decreases to 9.9 eV while its intensity slightly increases. The detailed study

(31) Hirst, J. D.; Hirst, D. M.; Brooks, C. L., III *J. Phys. Chem.* **1996**, *100*, 13487.
(32) Oliveros, E.; Riviere, M.; Teichteil, C.; Malrieu, J. P. *Chem. Phys. Lett.* **1978**, *57*, 220.
(33) Sobolewski, A. L. *J. Photochem. Photobiol.* **1995**, *89*, 89.
(34) Nielsen, E. B.; Schellman, J. A. *J. Phys. Chem.* **1967**, *71*, 2297.
(35) Dudik, J. M.; Johnson, C. R.; Asher, S. A. *J. Phys. Chem.* **1985**, *89*, 3805.

Table 4. Calculated and Experimental Excitation Energies (eV), Oscillator Strengths, Dipole Moments μ (D), Spatial Extension $\langle r^2 \rangle$ (au), and Transition Moment Directions (deg) for the Excited Singlet and Triplet States in *N*-Methylformamide

	excitation energies					oscil str		TM dir[a]
state	CAS	PT2	exp	μ	$\langle r^2 \rangle$	tw[g]	exp	tw[g]
$1^1A'$(G.S.)				4.07	55			
$1^1A''(n \rightarrow \pi^*)$	8.64	5.52	5.5[c]	2.24	61	0.002	0.002[f]	
$2^1A''(3a'' \rightarrow 3s)$	7.75	6.08		5.90	96	0.007		
$2^1A'(13a' \rightarrow 3s)$	8.21	6.51	6.5[e]	6.11	100	0.003	0.02[b]	+17
$3^1A'(\pi \rightarrow \pi^*)$	10.41	6.71	7.0[e]	6.17	59	0.315	0.21[f]	−38
$3^1A''(3a'' \rightarrow 3p_y)$	8.68	7.08		5.48	127	0.007		
$4^1A''(13a' \rightarrow 3p_z)$	8.96	7.12		1.00	118	0.001		
$4^1A'(3a'' \rightarrow 3p_z)$	8.30	7.13	7.2[e]	0.84	132	0.025		+3
$5^1A'$ $(13a' \rightarrow 3p_y)$	8.85	7.29	7.3[e]	8.34	118	0.017		+46
$5^1A''(3a'' \rightarrow 3p_x)$	8.88	7.37		6.92	135	0.008		
$6^1A'(13a' \rightarrow 3p_x)$	8.65	7.38	7.4[e]	0.25	166	0.009		−22
$6^1A''(3a'' \rightarrow 3d_{z^2})$	9.44	7.97		7.71	226	0.001		
$7^1A'(3a'' \rightarrow 3d_{xz})$	8.90	8.08		8.30	230	0.003		+33
$8^1A'(13a' \rightarrow 3d_{z^2})$	9.36	8.12		7.37	228	0.004		+34
$7^1A''(3a'' \rightarrow 3d_{xy})$	9.42	8.18		16.91	206	0.001		
$9^1A'(3a'' \rightarrow 3d_{yz})$	9.23	8.19		15.85	212	0.012		−59
$10^1A'(13a' \rightarrow 3d_{x^2-y^2})$	9.42	8.19		10.76	210	0.015		−2
$8^1A''(3a'' \rightarrow 3d_{x^2-y^2})$	9.47	8.22		20.88	197	0.000001		
$9^1A''(13a' \rightarrow 3d_{xz})$	9.69	8.23		12.53	210	0.00001		
$11^1A'(13a' \rightarrow 3d_{xy})$	9.44	8.24		16.15	205	0.002		+28
$10^1A''(13a' \rightarrow 3d_{yz})$	9.90	8.25		12.69	193	0.001		
$11^1A''(2a'' \rightarrow 3s)$	11.20	9.43		6.50	97	0.019		
$12^1A'(\pi \rightarrow \pi^*)$	14.01	9.70	9.9[b]	5.11	56	0.102	0.1[b]	+54
$1^3A''(n \rightarrow \pi^*)$	6.98	5.35		1.95	50			
$1^3A'(\pi \rightarrow \pi^*)$	6.96	5.42		4.37	52			
$2^3A''(3a'' \rightarrow 3s)$	6.29	6.04		5.86	93			
$2^3A'(13a' \rightarrow 3s)$	7.34	6.54		5.97	97			

[a] The molecule is placed in the *xy* plane (C_s symmetry). The convention used places the *y* axis along the CO bond and the nitrogen in the fourth quadrant. The positive angles are defined clockwise from the *y* axis in the first quadrant as in ref 9. See Figure 1. [b] Data from the crystal spectrum of propanamide. Reference 9. [c] Estimated value for methylacetamide in nonpolar solvent. In water the band appears near 5.7 eV. References 9 and 34. [d] Out-of-plane polarized transition in the gas phase. Reference 9. [e] Vacuum transition for *N*-methylformamide, ref 28. [f] Estimated values in solution. References 9 and 34. [g] This work.

of the crystal spectrum of propanamide performed recently by Clark[9] provides also accurate transition moment directions for the different transitions. Table 3 includes the computed and experimental transition moment directions, using the convention outlined in Figure 1. The experimental values for the valence $\pi \rightarrow \pi^*$ states of propanamide are −35° and +46° (−72°), respectively. The values in parentheses report the second possibility consistent with the observed spectra. Our computed values for the NV_1 and NV_2 transitions, −31° and +52°, respectively, are in agreement with the experimental values. It appears that the crystal effects do not strongly distort the transition moment directions for the valence states. Our calculations are also consistent with pervious INDO/S calculations by Clark[9] which have been used to select the correct angles. We also note that the observed and computed polarization angles for the R_1 band in propanamide, +75° and −38° (+4°), respectively, are almost orthogonal and deserve several comments. The R_1 transition is considered to be a Rydberg transition. Traditionally, it has been asserted that Rydberg transitions do not appear in condensed phases.[5] This does not seem to be true always. Rydberg states have been observed as weak shoulders in condensed phases[36] and even in solid phases or films.[9,37] Solute−solvent interactions will, however, perturb such Rydberg states and therefore transition moment directions measured in gas and in solid phases might be difficult to compare. Comparing the polarization directions with the data for formamide and acetamide, we also find that the transition moments of the valence states are preserved (±10°). In contrast, the polarization direction of the R_1 state changes drastically.

(36) Ilich, P.; Sedarous, S. S. *Spectrosc. Lett.* **1994**, *27*, 1023.
(37) Albinsson, B.; Nordén, B. *J. Phys. Chem.* **1992**, *96*, 6204.

2. Secondary Amides: *N*-Methylformamide and *N*-Methylacetamide. The experimental gas-phase spectrum of *N*-methylformamide[28] presents a broad, structured band system ranging from 7.0 to 7.6 eV. The absorption maximum is a sharp peak at 7.4 eV. A complete assignment of all observed features is difficult to perform. The computed value for the excitation energy to the valence $\pi \rightarrow \pi^*$ NV_1 state is 6.71 eV with an oscillator strength of 0.315. The computed excitation energy is ≈0.7 eV too low compared to the experimental observation. Such a large error is very much unlikely and suggests that the experimental spectrum has been misinterpreted. Moreover, this discrepancy has also been observed in semiempirical calculations,[28] but has been attributed to the limitations of method. By comparing the spectra of acetamide and *N*-methylacetamide we find that the $\pi \rightarrow \pi^*$ excitation energy decreases ≈0.5 eV. In formamide, a smaller molecule, the effect of the substitution may be even larger and therefore expect to find the NV_1 state close to 6.9 eV. It appears that the valence $\pi \rightarrow \pi^*$ NV_1 state cannot be assigned to be one of the sharp peaks observed in the range from 7.1 to 7.5 eV and it may be hided in the low-energy side of the broad band. A more detailed gas-phase spectrum of *N*-methylformamide is required to solve the ambiguity in the assignment.

The gas-phase spectrum of *N*-methylacetamide[28] differs from that of *N*-methylformamide in that two well-separated bands are observed in the spectrum from 6.5 to 7.8 eV—one broad band centered around 6.8 eV and one sharp peak at 7.7 eV. The computed excitation energies for the valence $\pi \rightarrow \pi^*$ states are 6.76 and 9.60 eV, with oscillator strengths of 0.279 and 0.179, respectively. The result of 6.76 eV perfectly matches with the observed band maximum at 6.8 eV. Note also that the computed energy for the NV_1 state is 0.05 eV higher than

Table 5. Calculated and Experimental Excitation Energies (eV), Oscillator Strengths, Dipole Moments μ (D), Spatial Extension $\langle r^2 \rangle$ (au), and Transition Moment Directions (deg) for the Excited Singlet and Triplet States in *N*-Methylacetamide

	excitation energies						oscil str			TM dir[a]
state	CAS	PT2	exp	CI[b]	μ	$\langle r^2 \rangle$	tw[g]	exp	CI[b]	tw[g]
$1^1A'$(G.S.)					4.14	68				
$1^1A''(n \rightarrow \pi^*)$	8.20	5.49	5.5[c]	5.85	1.90	63	0.001	0.002[f]		
$2^1A''(4a'' \rightarrow 3s)$	7.45	5.96			5.10	111	0.005			
$2^1A'(16a' \rightarrow 3s)$	7.96	6.22	6.3[e]	5.83	4.35	112	0.014	0.02[d]	0.010	−84
$3^1A'(\pi \rightarrow \pi^*)$	10.00	6.76	6.8[e]	8.19	6.41	68	0.279	0.30[f]	0.167	−42
$4^1A'(4a'' \rightarrow 3p_z)$	8.48	6.93		7.13	1.01	148	0.019		0.046	−44
$5^1A'(16a' \rightarrow 3p_y)$	8.54	6.98			4.28	148	0.007			+52
$3^1A''(4a'' \rightarrow 3p_y)$	8.34	7.02			6.43	155	0.007			
$6^1A'(16a' \rightarrow 3p_x)$	8.67	7.03	7.1[e]	6.80	0.25	166	0.006		0.015	+39
$4^1A''(16a' \rightarrow 3p_z)$	8.65	7.11		7.00	0.45	152	0.000001		0.037	
$5^1A''(4a'' \rightarrow 3p_x)$	8.44	7.12			4.69	158	0.002			
$6^1A''(16a' \rightarrow 3d_{yz})$	9.34	7.71			9.02	230	0.00001			
$7^1A'(16a' \rightarrow 3d_{x^2-y^2})$	9.19	7.74	7.7[e]	7.29	12.88	222	0.012		0.004	−22
$8^1A'(16a' \rightarrow 3d_{z^2})$	9.31	7.75		7.37	7.37	228	0.003		0.015	+33
$9^1A'(16a' \rightarrow 3d_{xy})$	9.34	7.76		7.53	9.87	233	0.003		0.001	+48
$7^1A''(4a'' \rightarrow 3d_{z^2})$	9.04	7.85			7.71	226	0.002			
$8^1A''(16a' \rightarrow 3d_{xz})$	9.40	7.86			13.38	249	0.00001			
$9^1A''(4a'' \rightarrow 3d_{x^2-y^2})$	9.21	7.90			22.02	237	0.0001			
$10^1A'(4a'' \rightarrow 3d_{xz})$	9.29	7.91		7.93	8.30	230	0.005		0.029	−62
$10^1A''(4a'' \rightarrow 3d_{xy})$	9.24	7.94			25.28	217	0.0001			
$11^1A'(4a'' \rightarrow 3d_{yz})$	9.52	7.98		8.02	13.57	226	0.032		0.031	−17
$11^1A''(3a'' \rightarrow 3s)$	10.75	9.04			5.95	113	0.012			
$12^1A'(\pi \rightarrow \pi^*)$	12.89	9.60	9.9[b]		4.67	65	0.179	0.1[d]		+39
$1^3A''(n \rightarrow \pi^*)$	7.27	5.22		5.61	1.86	65				
$1^3A'(\pi \rightarrow \pi^*)$	7.58	5.43		6.11	4.66	67				
$2^3A''(4a'' \rightarrow 3s)$	6.81	5.86			4.67	110				
$2^3A'(16a' \rightarrow 3s)$	7.12	6.30			3.59	111				

[a] The molecule is placed in the *xy* plane (C_s symmetry). The convention used places the *y* axis along the CO bond and the nitrogen in the fourth quadrant. The positive angles are defined clockwise from the *y* axis in the first quadrant as in ref 9. See Figure 1. [b] Selected CI results. Reference 38. [c] Value for *N*-methylacetamide in nonpolar solvents. In water the band appears near 5.7 eV. References 9, 34 and 35. [d] Estimated values for propanamide from ref 9. [e] Vacuum transition for *N*-methylacetamide. Reference 28. In water the $\pi \rightarrow \pi^*$ band appears at 6.6 eV.[35,46] [f] Estimated values in solution. References 9 and 34. [g] This work.

in *N*-methylformamide. The low-lying $n \rightarrow \pi^*$ and $16a' \rightarrow 3s$ states appear to overlap the $\pi \rightarrow \pi^*$ band in the experimental spectra. Finally, three assignments have been made for the Rydberg states. The $6^1A'$ ($16a' \rightarrow 3p_x$) state computed at 7.03 eV is assigned to the weak feature observed at 7.1 eV. Both the computed intensity and the fact that this state (HOMO $\pi \rightarrow 3p_x$) remains strong in the different molecules suggest the assignment. More convincingly, the sharp 7.7-eV peak is assigned to be the $7^1A'$ ($16a' \rightarrow 3d_{x^2-y^2}$) state computed at 7.74 eV. This state also seems to keep its intensity in the other molecules.

Table 5 contains the comparison of the present values to the selected CI results by Nitzsche and Davidson.[38] Their results are comparable to the CASPT2 ones for the Rydberg transitions. The excitation energy for the valence NV_1 state, 8.19 eV, is undoubtedly too high, and is mainly due to the strong mixing of valence and Rydberg states.

3. Tertiary Amides: *N*,*N*-Dimethylformamide. To observe the effect of an additional alkyl substitution on the nitrogen we also computed the spectrum of *N*,*N*-dimethylformamide. Both Hunt and Simpson[10] and Kaya and Nagakura[28] report the experimental gas-phase spectrum up to 8.0 eV. Two well-separated bands are observed—one broad and intense band centered around 6.4 eV and a second, less broad band at 7.8 eV. The 6.4-eV band corresponds to the valence $\pi \rightarrow \pi^*$ NV_1 transition. Hunt and Simpson[10] assigned the 7.8-eV band to the second valence $\pi \rightarrow \pi^*$, NV_2 transition, and, over the years, it has also been believed to correspond to the second $\pi \rightarrow \pi^*$ valence state of the peptide chromophore in proteins.[1] This assignment is, however, not correct in the light of the present calculations. The NV_2 state is computed at 9.73 eV. Moreover, the effect of the additional methyl group is small: The excitation energy is 0.03 and 0.13 eV higher than in *N*-methylformamide and *N*-methylacetamide, respectively. Therefore, we assigned the intense 7.5- and 7.8-eV bands to the vertical transition to the $8^1A'(16a' \rightarrow 3d_{yz})$ and $10^1A'(16a' \rightarrow 3d_{x^2-y^2})$ Rydberg states, respectively.

4. General Trends. In general, it has been observed that the computed oscillator strengths for the valence and Rydberg transitions are qualitatively correct but may differ considerably from experiment on an absolute scale for the following reasons. Typically, the valence bands have vibrational progressions ranging from the band origin to the maximum and the tail of the band is due to differences in the equilibrium geometries of the excited state with respect to the ground-state geometry. Such long progressions are hardly seen for Rydberg states. However, valence and Rydberg bands are often superimposed. Hence, a proper assignment is usually difficult. The computed oscillator strengths for the NV_1 state range from 0.2 to 0.3 and the computed intensities for the Rydberg states are in general less than 0.1. In general, the observed bands in the spectra have similar intensities. This is, however, only true for gas-phase spectra, and it is due to the sharpness of the Rydberg band. This fact led Hunt and Simpson[10] to view the 7.8-eV band in *N*,*N*-dimethylformamide as being due to a valence and not a Rydberg state. A similar situation has been found previously in formaldehyde and acetone.[7,39] These molecules have a similar electronic structure as the amides except for the presence of a second π orbital (2a′ in formamide) in amides. The valence $\pi \rightarrow \pi^*$ NV_2 states can be viewed as a localized intracarboxyl excitation, and, therefore, it can be expected to be similar in both type of systems. This is true for the computed vertical excitation energies, 9.77 and 9.16 eV in formaldehyde and

(38) Nitzsche, L. E.; Davidson, E. R. *J. Am. Chem. Soc.* **1978**, *100*, 7201.

Table 6. Calculated and Experimental Excitation Energies (eV), Oscillator Strengths, Dipole Moments μ (D), Spatial Extension $\langle r^2 \rangle$ (au), and Transition Moment Directions (deg) for the Excited Singlet and Triplet States in *N*,*N*-dimethylformamide

	excitation energies					oscil str		TM dir[a]
state	CAS	PT2	exp[b]	μ	$\langle r^2 \rangle$	tw[f]	exp	tw[f]
$1^1A'$(G.S.)				4.20	71			
$1^1A''(n \rightarrow \pi^*)$	8.62	5.64	5.5	2.87	70	0.001	0.002[d]	
$2^1A''(4a'' \rightarrow 3s)$	7.67	5.92	5.9	1.57	119	0.005		
$2^1A'(16a' \rightarrow 3s)$	8.43	6.48		4.22	117	0.002	0.02[c]	+6
$3^1A'(\pi \rightarrow \pi^*)$	8.51	6.50	6.4	6.80	76	0.365	0.30[d]	−39
$4^1A'(4a'' \rightarrow 3p_z)$	8.28	6.55	6.4	1.13	148	0.004		−77
$3^1A''(4a'' \rightarrow 3p_x)$	8.22	6.63		1.21	157	0.002		
$4^1A''(4a'' \rightarrow 3p_y)$	8.36	6.77	6.7	1.19	162	0.001		
$5^1A''(16a' \rightarrow 3p_z)$	8.68	6.81	6.9	2.64	123	0.002		
$5^1A'(16a' \rightarrow 3p_y)$	8.90	7.09	7.1	1.34	152	0.010		+33
$6^1A''(4a'' \rightarrow 3d_{xy})$	8.52	7.16		10.61	215	0.00001		
$6^1A'(16a' \rightarrow 3p_x)$	9.02	7.20	7.2	1.30	161	0.004		+81
$7^1A''(4a'' \rightarrow 3d_{z^2})$	8.79	7.24		6.42	203	0.0001		
$8^1A''(16a' \rightarrow 3d_{xz})$	9.57	7.25		4.90	176	0.00001		
$9^1A''(4a'' \rightarrow 3d_{x^2-y^2})$	8.65	7.32		16.35	218	0.003		
$7^1A'(4a'' \rightarrow 3d_{xz})$	8.99	7.37	7.4	5.39	217	0.005		+85
$8^1A'(4a'' \rightarrow 3d_{yz})$	9.07	7.48	7.5	10.09	220	0.046		−59
$10^1A''(16a' \rightarrow 3d_{yz})$	9.29	7.66		12.69	193	0.001		
$9^1A'(16a' \rightarrow 3d_{z^2})$	9.48	7.76		7.52	207	0.003		+52
$10^1A'(16a' \rightarrow 3d_{x^2-y^2})$	9.47	7.84	7.8	5.95	220	0.014		−15
$11^1A'(16a' \rightarrow 3d_{xy})$	9.54	7.94		7.65	225	0.006		+70
$11^1A''(3a'' \rightarrow 3s)$	11.16	9.37		1.84	118	0.014		
$12^1A'(\pi \rightarrow \pi^*)$	11.58	9.73	9.9[c]	5.53	75	0.162	0.1[d]	+41
$1^3A''(n \rightarrow \pi^*)$	7.74	5.06	5.00[e]	2.14	65			
$1^3A'(\pi \rightarrow \pi^*)$	8.03	5.41		4.73	67			
$2^3A''(4a'' \rightarrow 3s)$	7.43	5.88		1.52	118			
$2^3A'(16a' \rightarrow 3s)$	7.66	6.57		5.66	116			

[a] The molecule is placed in the *xy* plane (C_s symmetry). The convention used places the *y* axis along the CO bond and the nitrogen in the fourth quadrant. The positive angles are defined clockwise from the *y* axis in the first quadrant as in ref 9. See Figure 1. [b] Vacuum transition for *N*,*N*-dimethylformamide, refs 10 and 28. [c] Data from the crystal spectrum of propanamide. Reference 9. [d] Estimated values in solution. References 9 and 34. [e] Trapped electron spectrum of *N*,*N*-dimethylformamide in the gas phase. Reference 30. [f] This work.

Table 7. Calculated CASPT2 Excitation Energies (eV) and Oscillator Strengths (*f*) for the Excited Singlet States of the Studied Molecules

state	PT2	*f*	PT2	*f*	PT2	*f*
	formamide		acetamide		propanamide	
$^1A''(n \rightarrow \pi^*)$	5.61	0.001	5.54	0.001	5.48	0.001
$^1A'(\pi \rightarrow \pi^*)$	7.41	0.371	7.21	0.292	7.28	0.346
$^1A'(\pi \rightarrow \pi^*)$	10.50	0.131	10.08	0.179	9.95	0.205
	N-methylformamide		*N*-methylacetamide			
$^1A''(n \rightarrow \pi^*)$	5.52	0.002	5.49	0.001		
$^1A'(\pi \rightarrow \pi^*)$	6.71	0.315	6.76	0.279		
$^1A'(\pi \rightarrow \pi^*)$	9.70	0.102	9.60	0.179		
	N,*N*-dimethylformamide					
$^1A''(n \rightarrow \pi^*)$	5.64	0.001				
$^1A'(\pi \rightarrow \pi^*)$	6.50	0.365				
$^1A'(\pi \rightarrow \pi^*)$	9.73	0.162				

acetone, respectively, and between 10.5 and 9.6 eV in the amides. Both in formaldehyde[7] and in acetone[39] detailed studies on potential energy curves of the valence and Rydberg states as a function of the C−O length coordinate were performed. The valence $\pi \rightarrow \pi^*$ state (NV_2) has been shown to decrease in energy to 7.84 and 7.42 eV in formaldehyde and acetone, respectively, when the C−O band distance is increased by 0.33 and 0.10 Å, respectively. The state is also proposed to have a short lifetime and therefore to appear in the spectrum as a diffuse background beneath the experimentally resolved transitions to the Rydberg states.[39] It is, however, the direct or indirect coupling between this valence state and the different Rydberg states that is responsible for the intensification of the otherwise weak and sharp Rydberg states. In the amides the mixing among the different states is even more pronounced than in formaldehyde or acetone due to the lower symmetry of the molecules. Direct observation of the $\pi \rightarrow \pi^*$ NV_2 state might be difficult due to the small Franck−Condon factors for the lower vibrational levels, if the formaldehyde and acetone models hold true for the amides.[2,7,39]

Table 7 lists the excitation energies and osillator strengths of the valence singlet excited states. The NV_1 band is the most intense transition in the spectrum. It can be characterized as HOMO → LUMO excitation. Typically, the HOMO has a large coefficient at the nitrogen atom. It can also be described as an intramolecular charge transfer transition. The population analysis reveals that a charge of 0.3−0.4 e^- has been transferred from the nitrogen to the CO group with respect to the ground-state population in all the molecules. The frequency of the transition will strongly depend upon the ionization potential of the $-NR_2$ group. The alkyl substituents on the nitrogen act as electron-withdrawing groups which destabilizes the second π orbital. This can be observed in the experimental ionization potential of methylamines, decreasing in the series $MeNH_2$, Me_2-

(39) Merchán, M.; Roos, B. O.; McDiarmid, R.; Xing, X. *J. Chem. Phys.* **1996**, *104*, 1791.

NH, and Me_3N: 8.89, 8.15, and 7.76 eV.[40] In addition, increasing the size of the alkyl chain will further lower the ionization potentials. Since the substituents also become more polarizable, states for which the nitrogen atom is charged[41] will be stabilized further. The ionization potentials for the ethylamines $EtNH_2$, Et_2NH, and Et_3N are 8.76, 7.85, and 7.11 eV. In conclusion, substitution on the nitrogen atom leads to a considerable stabilization of the NV_1 state with transition energies of 7.4, 7.0, and 6.5 eV for formamide, *N*-methylformamide, and *N*,*N*-dimethylformamide (cf. Table 7) and 7.4 and 6.8 eV for acetamide and *N*-methylacetamide, respectively. Taking *N*-methylacetamide as the best model for larger peptides, a further decrease of the excitation energy can be expected for larger substituents on the nitrogen atom. The early spectroscopic studies on proteins showed a high-intensity absorption band in the neighborhood of 6.5 eV which increased in intensity from smaller to larger oligopeptides.[42] This band is not seen in aliphatic amino acids and it can be easily related to the NV_1 ($\pi \rightarrow \pi^*$) transition in simple peptides. At a first approximation, the peptide group behaves as an isolated chromophore with additive intensities.[43,44] Other possibilities for the assignment of the 6.5-eV band in proteins can be discarded, as will be shown by our subsequent study on simple amino acids and peptides.[4] The band at 6.5 eV is also a clear characteristic of polyamides such as nylons and related polymers,[5,45] where the peptidic bonds are the unique chromophores.

The effect attaching alkyl groups to the carbon atom is, in general, opposite to that of alkylating the nitrogen atom, i.e. the energy of the NV_1 transition[5] increases slightly. This effect can be observed comparing acetamide to propanamide and *N*-methylformamide to *N*-methylacetamide (cf. Table 7). However, the substitution effect is less than 0.1 eV in both cases. The situation is different in formamide, where the computed excitation energy is 0.2 eV higher than in acetamide and can be rationalized in a qualitative way. The methyl group promotes the generation of a positive charge in the π system of an adjacent atom. Mulliken populations calculated for the ground state of the present molecules at the SCF level of approximation reveal the following net charges on nitrogen: −0.78 (formamide), −0.81 (acetamide), −0.81 (propanamide), −0.61 (*N*-methylformamide), −0.65 (*N*-methylacetamide), and −0.44 (*N*,*N*-dimethylformamide). The corresponding charges on the carbon atom attached to the oxygen are +0.35 (formamide), +0.57 (acetamide), +0.59 (propanamdie), +0.34 (*N*-methylformamide), +0.56 (*N*-methylacetamide), and +0.34 (*N*,*N*-dimethylformamide). Since the NV_1 transition is largely a nitrogen-to-carbon charge transfer, the excited state will be stabilized by the methyl effects decreasing the charge on nitrogen and increasing it on carbon as found by *N*-alkylations. *C*-alkylations, on the contrary, will destabilize the excited state. The effect can also be observed in the orbital energy (SCF level) of the HOMO (π) orbital. Its energy does not vary in the series formamide, acetamide, and propanamide (*C*-alkylation), but it is destabilized by 0.5 eV in *N*-methylformamide and *N*-methylacetamide, and by 2.0 eV in *N*,*N*-dimethylformamide. The orbital has a node on the carbon atom and therefore its energy it is not affected by substitutions on that atom. Formamide is an exception from these rules in that the lowest π^* orbital is localized on the CO group and 0.5 eV higher in energy as compared to acetamide and propanamide. Moreover, comparing formamide to acetamide, the electron-withdrawing effect upon *C*-alkylation is large (+0.22e). Thus, the stabilization of the antibonding orbital in acetamide and propanamide is due to the strong delocalization when attaching the alkyl substituent.

Robin[5] also observed a reduction of intensity of the NV_1 transition in various alkylated amides as compared to formamide. This is also a consequence of the nature of the HOMO and LUMO orbitals. In formamide both orbitals have large spatial overlap because the LUMO π^* orbital is localized. The opposite situation occurs on the remaining amides, where a decrease of the transition intensity can be explained by the lack of spatial overlap between the orbitals. In summary, the expected *N*-alkylation and *C*-alkylation effects are fulfilled in the studied amides except in formamide due to the absence of any type of substituents.

Finally, the Q band of amides can be assigned as the valence $\pi \rightarrow \pi^*$ NV_2 transition, computed between 9.6 and 10.5 eV in the different molecules. The analysis of the wave function reveals that it is not strictly an intracarboxylic transition. The contribution to the wave function of the HOMO-1 → LUMO $\pi \rightarrow \pi^*$ single excitation is about 60%, but the double excitation HOMO,HOMO → LUMO,LUMO $(\pi)^0 \rightarrow (\pi^*)^2$ contributes about 25%, with a subsequent transfer of charge from nitrogen to carbon. As discussed earlier in this section, this state is thought to decrease in energy when increasing the CO bond length. In addition, in gas-phase Rydberg and valence states are interfering thus leading to states of composite character and complex band structures. In solid and liquid phase, where Rydberg states cannot be observed, the electronic spectra of amides expose a single intense band close to 9.9 eV.[5] It has been suggested that it was related to the conduction band of the solid, but an alternative explanation is that the interaction among the valence and Rydberg states is greatly reduced in solids and therefore the NV_2 band increases in intensity.

4. Summary and Conclusions

With the general aim to characterize the origin of electronic spectra of proteins, the present paper discusses the absorption spectra of a series of simple amides. To this end, we computed the vertical electronic gas-phase absorption spectra of three primary amides (formamide, acetamide, and propanamide), two secondary amides (*N*-methylformamide and *N*-methylacetamide), and one tertiary amide (*N*,*N*-dimethylformamide). The results are compared to the available experimental information. The ground-state geometries of the present molecules were optimized at the MP2 level of approximation. Excited states were studied by the CASSCF/CASPT2 method. The calculations include a large number of singlet and triplet valence and Rydberg excited states.

The computed spectra obtain for each of the molecules one intense valence $\pi \rightarrow \pi^*$ NV_1 transition placed between 6.5 and 7.4 eV and a second weak valence $\pi \rightarrow \pi^*$ NV_2 transition at 9.6−10.5 eV. Attaching an alkyl group to the nitrogen atom strongly decreases the energy of the $\pi \rightarrow \pi^*$ transitions, while the alkyl substitution on the carbon leads to a small increase of the energy of the first $\pi \rightarrow \pi^*$ valence band. These rules do not apply to the smallest amide, formamide, due to the localization of the LUMO orbital in the absence of substituents. The intense NV_1 band can be related to the characteristic band observed at 6.5 eV in the protein's spectra. This band shows an increasing intensity with the number of oligomers, suggesting

(40) Aue, D. H.; Webb, H. M.; Bowers, M. T. *J. Am. Chem. Soc.* **1976**, *98*, 311.
(41) Serrano-Andrés, L.; Merchán, M.; Roos, B. O.; Lindh, R. *J. Am. Chem. Soc.* **1995**, *117*, 3189.
(42) Wetlaufer, D. B. Ultraviolet spectra of proteins and amino acids. In *Advances in Protein Chemistry*; Anfinsen, C. B., Anson, M. L., Bailey, K., Edsall, J. T., Eds.; Academic Press: New York, 1962; Vol. 17.
(43) Goldfarb, A. R. *J. Biol. Chem.* **1952**, *201*, 317.
(44) Saidel, L. J. *Arch. Biochem. Biophys.* **1955**, *56*, 45.
(45) Onari, S. *J. Appl. Phys.* **1970**, *9*, 227.
(46) Basch, H.; Robin, M. B.; Kuebler, N. A. *J. Chem. Phys.* **1967**, *47*, 1201.

the approximate additive character of the absorption taking place in the amide group when acting as the peptide chromophore. In the authors opinion, the second intense band in electronic spectra of proteins has been misinterpreted as being due to the second valence $\pi \rightarrow \pi^*$ transition. The latter has been computed at energies ranging from 9.6 to 10.5 eV.

The $n \rightarrow \pi^*$ transition from the oxygen lone pair to the CO antibonding orbital was computed at ≈5.5 eV for all species. The $n \rightarrow \pi^*$ excitation energies show only slight sensitivity to the length of the alkyl chain and the center of substitution. The general trends are the opposite to those observed for $\pi \rightarrow \pi^*$ transitions.

We studied also a number of Rydberg states and made tentative assignments for some of the most intense bands. We find that the R_1 Rydberg is composed of the n and HOMO π transitions to the 3s orbital on the low-energy side of the first $\pi \rightarrow \pi^*$ band. On the other hand, the R_2 Rydberg band at the high-energy side of the $\pi \rightarrow \pi^*$ band is shown to be composed either of 3p or 3d transitions ($^1A'$ symmetry) depending on the position of the valence band. These Rydberg bands had previously been confused with the NV_2 valence band, located at higher energies in the vertical spectrum.

In summary, the present calculations clearly describe the 6.5-eV band found in protein spectra as the low-lying $\pi \rightarrow \pi^*$ transition originated from the peptide bond but did not reveal any suitable candidate, i.e. an intense valence state, to explain the second intense band observed in electronic spectra of proteins at 7.5 eV. This question will be addressed in more detail in a subsequent publication including calculations on simple models of dipeptides.

Acknowledgment. The research reported in this paper has been supported by a grant from the Swedish Natural Science Research Council (NFR), by IBM Sweden under a joint study contract, by project PB94-0986 of the Dirección General de Investigación Científica y Técnica of Spain, and by the European Commission through the TMR programme. Luis Serrano acknowledges a post doctoral grant from the DGICYT of the Ministerio de Educación y Ciencia of Spain. The authors are indebted to Prof. Björn Roos for helpful comments and discussions on the present work.

Supporting Information Available: Tables containing the MP2/6-31G* ground state optimized geometries for formamide, acetamide, propanamide, *N*-methylformamide, *N*-methylacetamide, and *N*,*N*-dimethylformamide in C_s symmetry and the exponents and optimized coefficients of the Rydberg basis functions for each one of the molecules (5 pages). See any current masthead page for ordering and Internet access instructions.

JA961996+